Non-Thermal Annealing of Gamma Irradiated GaN HEMTs with Electron Wind Force

ECS Journal of Solid State Science and Technology, 2022 **11** 075002
2162-8777/2022/11(7)/075002/6/$40.00 © 2022 The Electrochemical Society ("ECS"). Published on behalf of ECS by IOP Publishing Limited

Non-Thermal Annealing of Gamma Irradiated GaN HEMTs with Electron Wind Force

Md Abu Jafar Rasel,[1] Sergei Stepanoff,[2] Aman Haque,[1,z] Douglas E. Wolfe,[2] Fan Ren,[3] and Stephen Pearton[4]

[1]*Department of Mechanical Engineering, Penn State University, University Park, PA 16802, United States of America*
[2]*Department of Materials Science & Engineering, Penn State University, University Park, PA 16802, United States of America*
[3]*Department of Chemical Engineering, University of Florida, Gainesville, FL 32611, United States of America*
[4]*Department of Material Science and Engineering, University of Florida, Gainesville, FL 32611, United States of America*

Radiation damage mitigation in electronics remains a challenge because the only established technique, thermal annealing, does not guarantee a favorable outcome. In this study, a non-thermal annealing technique is presented, where electron momentum from very short duration and high current density pulses is used to target and mobilize the defects. The technique is demonstrated on ^{60}Co gamma irradiated (5×10^6 rad dose and 180×10^3 rad h^{-1} dose rate) GaN high electron mobility transistors. The saturation current and maximum transconductance were fully and the threshold voltage was partially recovered at 30 °C or less. In comparison, thermal annealing at 300 °C mostly worsened the post-irradiation characteristics. Raman spectroscopy showed an increase in defects that reduce the 2-dimensional electron gas (2DEG) concentration and increase the carrier scattering. Since the electron momentum force is not applicable to the polymeric surface passivation, the proposed technique could not recover the gate leakage current, but performed better than thermal annealing. The findings of this study may benefit the mitigation of some forms of radiation damage in electronics that are difficult to achieve with thermal annealing.
 [DOI: 10.1149/2162-8777/ac7f5a]

Manuscript submitted May 22, 2022; revised manuscript received June 30, 2022. Published July 18, 2022.

AlGaN/GaN high electron mobility transistors (HEMTs) are attractive for high-power, high temperature, and high-frequency applications because of their high critical electric field and excellent transport properties compared to conventional Si and GaAs technologies.[1,2] Key to their superior electrical performance is the piezoelectric-induced channel formed by a high-density 2-dimensional electron gas (2DEG).[3] They have also gained considerable interest for use in extreme conditions such as radiation-harsh environments in space, aviation, defense, medicine, and nuclear power because of their higher threshold energy for atomic displacement.[4] However, radiation effect on the trap states is known to induce negative shift of the threshold voltage due to hole trapping in the barrier layer or the interface between the barrier and the channel layer.[5] Exposure of GaN HEMTs to radiation has been found to degrade saturation drain current, gate leakage, and extrinsic transconductance (G_m) due to the introduction of defects that act as scattering centers, leading to higher channel temperature and stress and thus decreasing operational reliability.[6–9] The extent of damage and the physics of evolution depends on the type and level of radiation dose as well as annealing temperatures.[10] The extent of recovery reported in the literature ranges from partial to none.[11]

Thermal annealing has been used predominantly to minimize defects in electronic materials and devices.[12–15] The findings are not very straightforward for ^{60}Co gamma radiation. The GaN HEMT literature has reported rearrangement and removal of the pre-existing and radiation induced defects/trap centers at annealing temperatures ranging from 100 °C–1000 °C and suggested higher temperatures for higher doses of irradiation.[6,11–14,16,17] At the same time, damage from 10^7 rad (60×10^3 rad h^{-1} dose rate) exposure is reported to be annealed marginally by prolonged storage at room temperature, with some permanent changes that deteriorated over time.[18,19] The fundamental principle behind thermal annealing is that the enhanced atomic vibration at higher temperatures induces mobility in defects to diffuse them towards elimination by recombination of primary defects or dissolution of defect complexes. The process is not straightforward for multi-layered materials with different thermal expansion coefficient since higher temperatures can increase thermo-elastic strain. Relaxation of this strain may actually increase the defect density in the channel, leading to a decrease in mobility.[12] In addition, the HEMT gate is Schottky type, and the barrier height is highly sensitive to thermally-induced reaction with the semiconductor.[20,21] This indicates the need for an alternative and preferably non-thermal process to anneal radiation damage in electronic materials and devices.

We explore the effectiveness of the electron wind force (EWF), which is purely mechanical in nature and derived from electron-defect interaction. The electron momentum is transferred to the defective atoms, which gives rise to the EWF. Depending on the electron momentum (which can be controlled by current density), the EWF can impart sufficient mobility to the defects to trigger annealing without any need for thermal vibration. The fundamental principle is the same as the concept of electro-migration damage,[22] where the uncontrollable temperature field arising from electron-lattice interaction leads to thermal runaway. In this study, we suppress the temperature field by passing current pulses with a very small duty cycle, allowing only the EWF to manifest. It is important to note that EWF is, by default, very specific to defects because it arises from electron-defect interaction only.[23] Therefore, if the temperature field is suppressed, EWF is expected to target only the defects to produce an annealing effect while leaving the lattice or ordered atoms alone. The concept has been applied to field effect transistors,[24] although DC current was used instead of pulsed currents.

The objective of this study is to explore the effectiveness of low duty cycle pulsed current on annealing gamma radiation damage in GaN HEMTs. Gamma rays primarily interact with electrons and may get absorbed, scattered, or produce electron-positron pairs.[25] The electrons generated by this process are known as Compton electrons. The radiation also creates Frenkel pairs and defect clusters that can migrate, recombine, or form complexes within materials.[26,27] A high-energy electron can trigger secondary electrons, which can cause displacement damage through non-ionizing energy loss.[28,29] If it has sufficient energy ($E > E_d$), it can knock off a nucleus of a lattice atom and create a stable trap or permanent defect. This typically acts as a recombination center which traps conducting electron or hole and thus reduces carrier concentration in the channel. Several research groups employed post-processing annealing to irradiated devices to return to their pre-irradiated state. Yadav et al. showed that low dose and high dose gamma irradiation cause a 10.6% and 62.3% decrease in diffusion length in GaN

[z]E-mail: mah37@psu.edu

HEMT, but after annealing at 250 °C, it was recovered by 66.7% and 22.6%, respectively.[11] The impact of electron injection (such as Scanning Electron Microscope beam) on irradiated devices has demonstrated the potential for reducing radiation-induced defects in electronic devices. Several other reports claim that the device performance was not fully recovered even after the high-temperature post-irradiation annealing except for partial recovery at a particular intermediate temperature after gamma irradiation.[15,30] Apart from thermal annealing after irradiation, novel current injection-enhanced annealing has been used in neutron-irradiated GaN LEDs.[31] The recovery of MOS structures and MOSFET dosimeters by thermal and current annealing to remove traps in the oxide layer and interfaces have been well studied.[32–34] These processes usually require a long annealing time at high temperatures.

Experimental

Commercially available (CGH60008D, Wolfspeed) dies were irradiated at room temperature to cobalt-60 γ-doses of 5×10^6 rad at the Radiation Science and Engineering Center at Penn State University. Samples were fixed within a 4″ Ø × 4″ tall iso-dose region inside the Gamma Cell and irradiated at a NIST traceable certified dose rate of 180×10^3 rad h^{-1}. The layer structure reported by the manufacturer included a ≈20 nm $Al_{0.22}Ga_{0.78}N$ barrier, ≈1 nm thick AlN interlayer, 1.4 μm GaN buffer, and 100 μm 4H–SiC substrate with a gate length of $L_g = 0.25$ μm. The HEMTs were in floating condition during radiation. The irradiated HEMTs were annealed at near-ambient temperature with the process schematically described in Fig. 1a. Here a DC power supply (Sorensen DCS100–12E) is used with a current pulse generator (Laser Controller, ED2P-AXA-0032) to apply up to 80 A current at as small as 20 micro-seconds pulse duration. To minimize the temperature, we used 20 micro-seconds pulses at 2 Hz frequency. The annealing process is carried out under an Optris PI 640 thermal microscope to track the temperature rise in real time. This is shown in Figs. 1b and 1c. The EWF-based annealing process took approximately 2 min with the temperature below 30 °C. The 640 × 480 pixels thermal microscope has 17 micrometers pixel pitch, which does not spatially resolve the HEMT gate. However, if the gate temperature increases, the heat flows to the GaN layer to raise the overall temperature of the HEMT die. Such die-averaged temperature rise can be detected with the microscope temperature sensitivity of 75 mK. Our temperature measurements are therefore only approximate in nature, but the low die average (<30 °C) suggests minimal heating. It is important to note that even at 80 A current, the very small pulse and low frequency enable near-room temperature operation and thus avoid thermal runway for the HEMT. In terms of power, the CGH60008D is rated 5 W for 20 V operation, whereas the average power supplied by one pulse at 2 Hz frequency with an amplitude of 80 A is only 8 mW. We also performed thermal annealing for 2 min at 300 °C to compare the outcomes with the proposed EWF-based annealing. Finally, the pristine, irradiated, and annealed (both EWF and thermal) HEMTs were electrically characterized with a temperature-controlled semiconductor parameter analyzer (Formfactor 11000). The degradation in electrical characteristics of the device is found to be permanent as no significant changes were detected over 3 months.

Results

Electrical characterization was performed at room temperature on the pristine, ^{60}Co gamma irradiated (5×10^6 rad), EWF-annealed (80 A, 20 μs, 2 Hz), and thermally annealed (300 °C, 2 min) HEMT specimens. All data presented are for 6 gate fingers, each with width and length of 0.25 and 200 microns respectively. Figure 2 shows the output and transfer curves at zero gate voltage. The radiation damage decreases the saturation current by 5.1%, which is recovered and enhanced beyond the pristine value for EWF-annealing. Similar results are seen for the transfer characteristics. We performed linear interpolation of the transfer curves to investigate the impact on the threshold voltage. This is shown in Fig. 3, where complete recovery of the threshold voltage is observed.

Gamma radiation is seen to degrade the trans-conductance (G_m), as shown in Fig. 4a. Here the typical bell shape is seen for the pristine device, which is significantly narrowed down (early collapse) by the radiation. The G_m collapse is ascribed to surface/interface and optical phonon scattering, even though pronounced roles of non-linear source and drain resistances and self-heating are suggested more recently.[35] Since the source and drain resistances are Ohmic in nature, EWF is expected to be effective in lowering them. Self-heating should not be a demarcation factor since the substrate is the same (SiC) in all cases. Therefore, we expect the transconductance degradation to be recovered by EWF-annealing. This is reflected in Fig. 4a. As shown in Fig. 4b, we did not see a major recovery in the leakage current. This is also expected because the EWF-annealing mechanism does not work for any insulating layer or interfaces. The HEMT used in this study employs a polymeric passivation layer for the external surface. It is well-known that leakage current depends on the radiation damage inflicted on the passivation-barrier, buffer-substrate interfaces as well as these layers.[1] Since the EWF is ineffective on non-conducting materials, the technique was unable to recover the leakage current. A slight increase in leakage current after EWF annealing can originate from the presence of surface traps in the gate-source/drain regions Si_3N_4/AlGaN interface generated due to a high electric field during electro-pulsing.[36]

Discussion

An important question is how conventional thermal annealing performs compared to the EWF-annealing data presented above. These two processes are fundamentally different because they use temperature induced atomic vibration and mechanical force

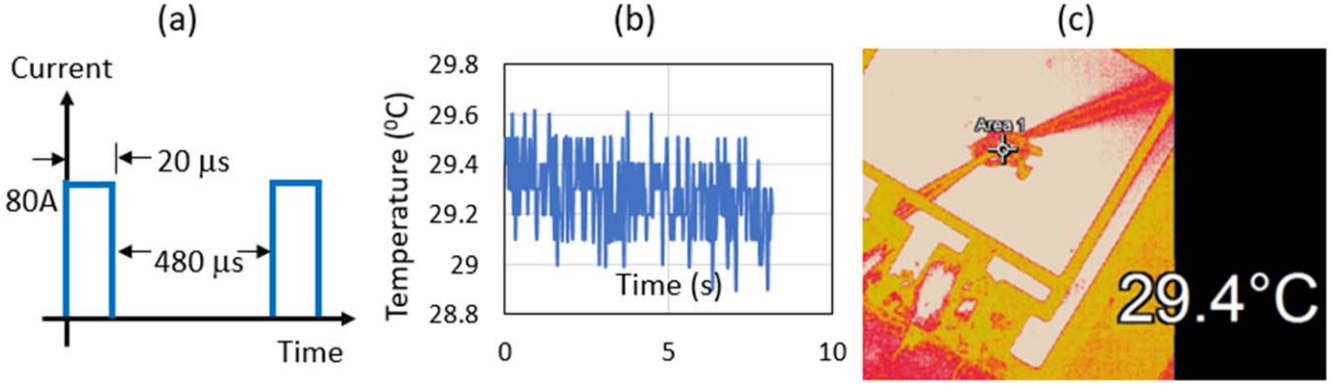

Figure 1. (a) EWF-based annealing process with electrical pulse parameters. (b) Temperature profile on the HEMT surface. (c) Thermal image of the HEMT during EWF annealing.

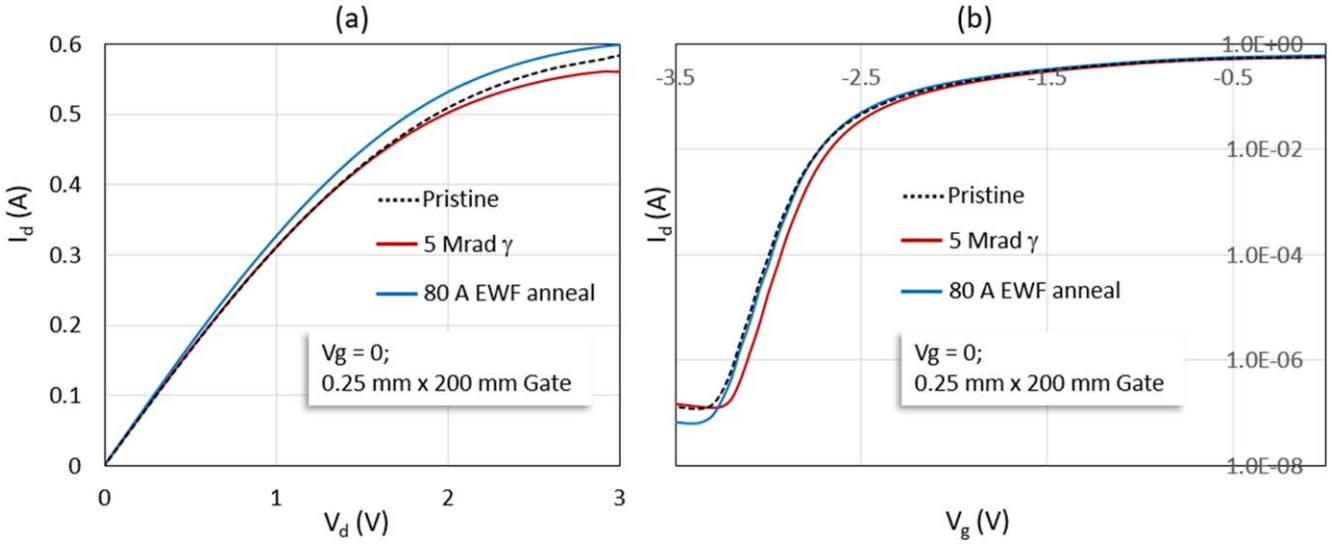

Figure 2. Effect of gamma irradiation doses and EWF-annealing on DC (a) output, I_{ds} - V_{ds} and (b) transfer, I_{ds} - V_g characteristics.

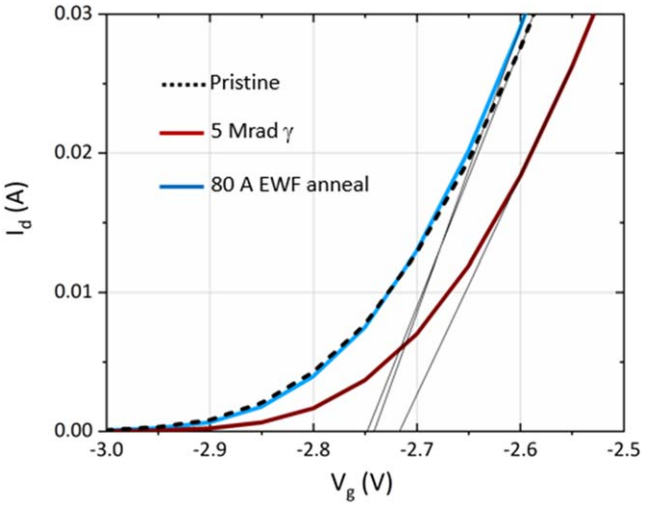

Figure 3. Threshold voltage changes due to gamma irradiation and EWF-annealing at zero gate voltage.

respectively to mobilize defective atoms. In thermal annealing, higher temperature implies higher defect mobility through increased atomic vibration amplitude. This influences temperature selection to anneal irradiated devices.[6,11–14,16,17] However, both lattice/ordered and defective atoms experience this vibration, making the atomic diffusion a random process. This is why conventional thermal annealing requires longer times to remove the defects. However, the critical factor is not time, but the thermo-mechanical stress generated by the temperature. For electronic devices, the multi-layered structure means large thermal mismatch strain, which may increase the defect density instead of decreasing it. EWF, on the other hand, is a purely mechanical force that pushes atoms via convection–diffusion (in the direction of electron flow). For conventional biasing, Joule heating is always associated with EWF. Therefore, the effectiveness of the proposed EWF-based annealing depends on (a) suppression of the temperature and (b) electrical conductivity of the material.

We performed thermal annealing at 300 °C in an argon environment. The duration was 2 min, the same amount for EWF annealing. The experimental results did not show any improvement in the output, transfer, transconductance or leakage characteristics. The saturation current decreased while the leakage current increased after thermal annealing, suggesting increased defect density at the AlGaN barrier. This may arise from the thermo-elastic relaxation in the AlGaN, which reduces the piezoelectric polarization in the material and, consequently, the 2DEG density.[37] Defects form due to AlGaN relaxation and provide a path for electrons to leak from the gate toward the drain contact, increasing gate leakage. Figure 5 shows the transfer function as well as the transconductance comparison between the EWF and thermal annealing techniques. Interestingly, the thermally annealed sample showed kinks in drain current near $V_g \approx -2$ V and -3 V. Along with the significant increase in the leakage current, the data suggests the generation of additional traps in the GaN buffer or AlGaN barrier layer.[38,39]

To obtain insights into the structural/crystal quality differences between the EWF and thermal annealing, we performed micro-Raman spectroscopy. Measurements were taken in a backscattering configuration with unpolarized detection, enabling the A_1 (LO) and E_2 (high) phonon modes of GaN to be measured simultaneously. It is known that the full-width at half-maximum (FWHM) of E_2 (high) phonon mode reflects the defect density in the crystal,[40] while any shift in the peak indicates the internal stress.[41,42] For higher spectral resolution, we used an 1800 g/mm grating along with a 100×, NA = 0.9 objective lens with a lateral spot size of $<1.0\ \mu$m. As shown in Fig. 6a, spectral mapping was performed with a step interval of 2 um across the device channels with an array of 11 x 19 points. Each line scan across the device channel was then analyzed to provide the mean and variance of the Raman FWHM at each position along the channel. Peak FWHM was determined by peak fitting the Raman spectra using a Lorentzian peak profile using the LabSpec6 software. Figure 6b indicates peak broadening happened after irradiation, indicating lower crystal quality and increased dislocation density.[43] Both thermal and EWF annealing improve GaN film quality, but EWF produced the narrowest FWHM.

An important point of discussion is the electro-pulsing parameters for the low temperature EWF annealing. The technique is expected to work with materials with electrons as the majority carriers. Thus, higher current density implies higher efficacy. Because traps have different depths or energy levels, their elimination may also need different current densities. The concern with very high current density is the increasing possibility of temperature increase leading to thermal runaway. Therefore, the studies should preferably be performed under temperature control or at least monitoring with a thermal microscope. In this study, we used the smallest pulse duration (20 μs) and frequency (2 Hz) to facilitate this. We performed the EWF annealing for up to 80 A current. The improvements were first noticed at 5 A. Between 5 and 80 A we did

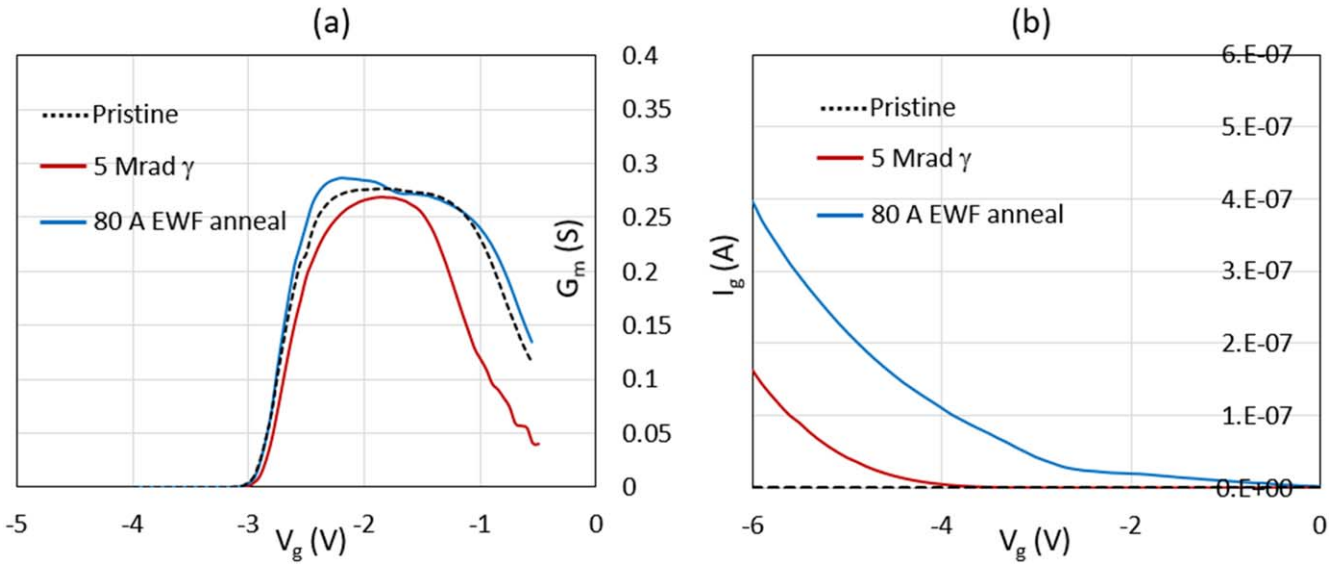

Figure 4. (a) Transconductance-gate voltage and (b) leakage current curves for the pristine, irradiated and EWF annealed HEMTs.

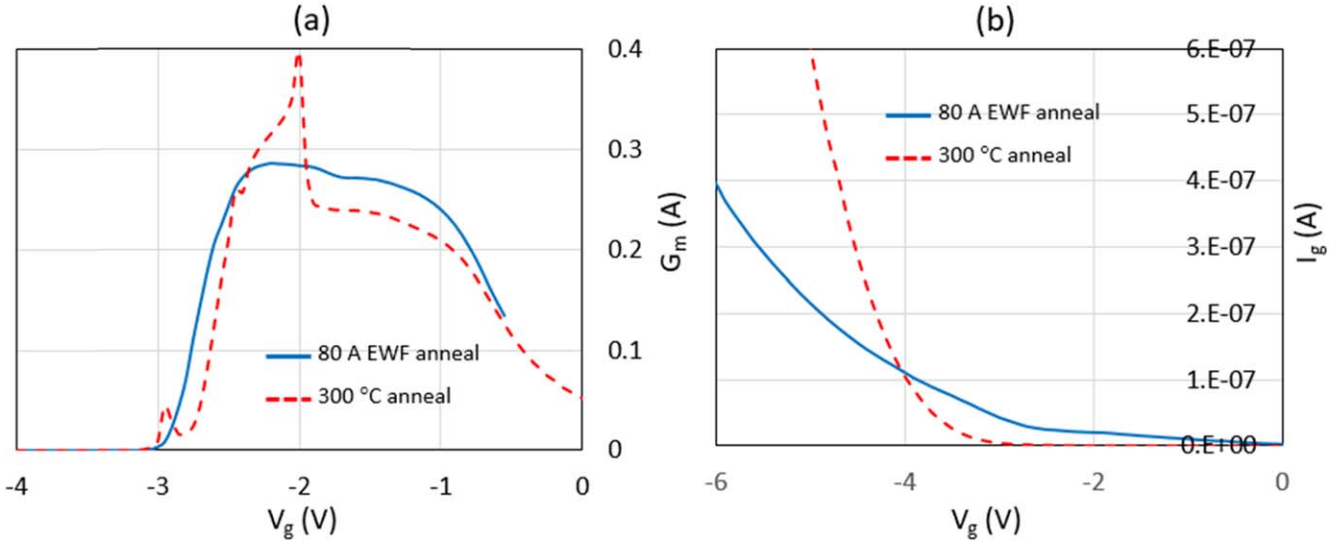

Figure 5. (a) Transconductance-gate voltage and (b) leakage current curves for EWF annealed HEMTs compared to conventional thermal annealing at 300 °C.

not see appreciable improvement. As shown in Fig. 7, distinct improvement was seen at 80 A. This suggests a different level of electro-pulse energy may be needed to interact with traps of different depths. It is important to note that these experimental parameters would strongly depend on the device type and details of the radiation environment. Therefore, it is important to conduct a comprehensive study of the electro-pulsing parameters and compare that with the gamma radiation literature. This will be conducted in the future.

Conclusions

Thermal annealing has been the only available technique in the literature. For multi-material, multi-layered systems, as in a transistor, the outcome is not always straightforward as high temperature can also create new defects. In this study, we demonstrate a non-thermal annealing scheme that should be attractive for electronic devices. The technique exploits EWF while suppressing Joule heating by applying high current density electrical pulses with very small duty cycle (4%). The EWF is a purely mechanical force that mobilizes the defective atoms, leaving the lattice/ordered atoms alone. This is possible because of the unique defect specificity of the EWF generation due to electron-defect interactions. Thermal annealing, on the other hand, involves uniform heating of both lattice/ordered and defective atoms to mobilize them through random diffusion. To examine our hypothesis, a comparative study between thermal and EWF annealing is performed on 5×10^6 rad gamma irradiated GaN HEMT. The EWF annealing could partially to fully recover the threshold voltage, transconductance, and saturation current. On the other hand, thermal annealing induced more defects and further degraded device performances. The findings are summarized in Table I.

The findings of this study will potentially benefit the microelectronic community, where the defect density in multi-material and multi-layered systems can strongly impact performance and reliability. Thermal annealing is a very well-established technique, but a non-thermal approach can be more beneficial. The proposed EWF-based annealing technique requires lower energy and processing times. It can be performed in-operando because there is no need to subject the device of interest to an oven as in thermal annealing. At the same time, the EWF is effective only for materials with electrons as majority carriers. Also, it may not be useful for the current leakage through the surface or interface of insulating layers.

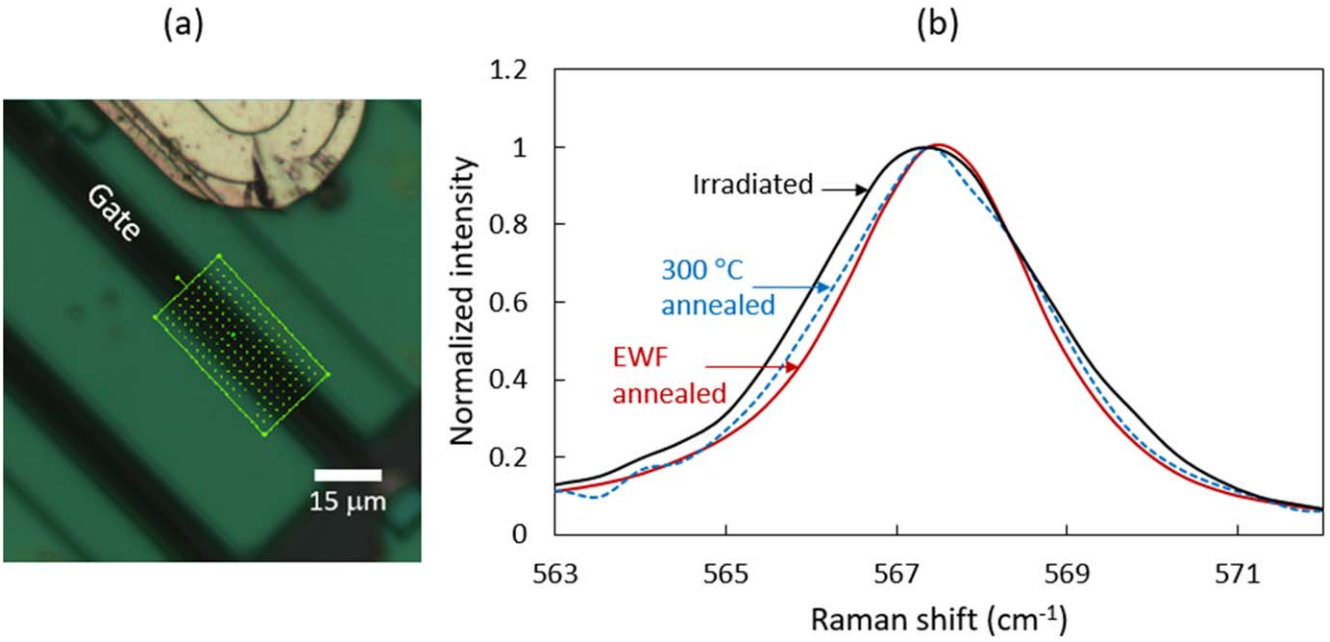

Figure 6. (a) Raman map grid on the GaN HEMT channel region to determine crystal quality. (b) E_2 (high) peak for the irradiated and annealed specimens.

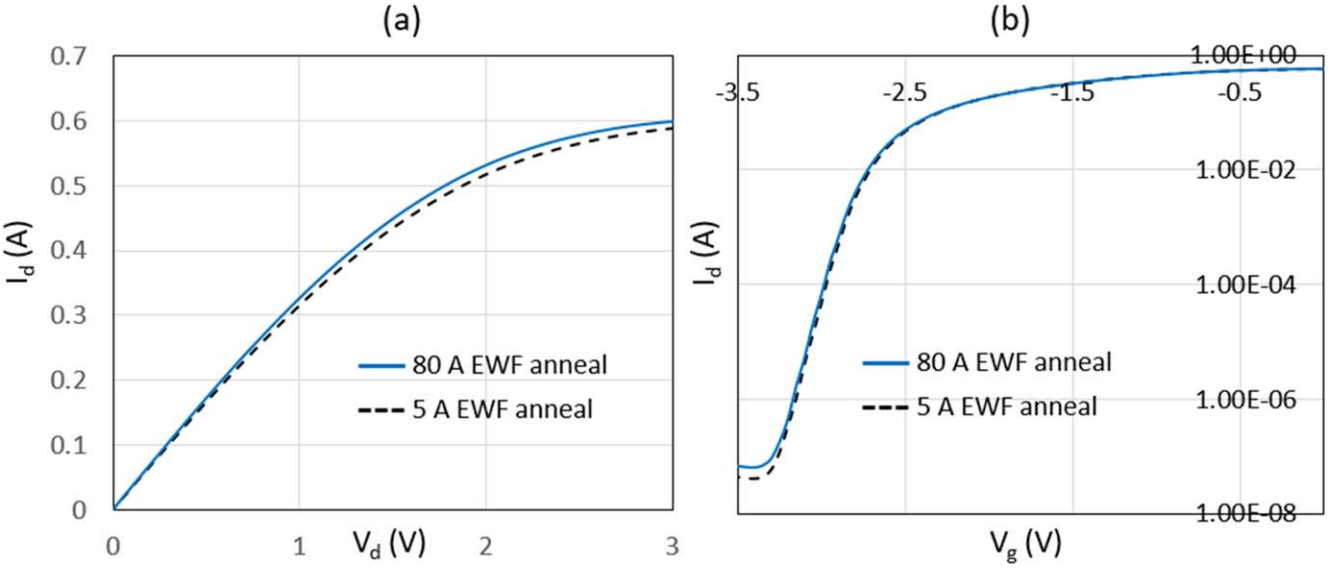

Figure 7. Effect of current density on (a) output and (b) transfer curves for EWF annealing for pulses with 20 μs duration and 2 Hz frequency.

Table I. Saturation drain current, threshold voltage, leakage current (at −5 V gate voltage), maximum transconductance, and average FWHM as a function of irradiation and two different annealing processes.

	Pre-Irradiated	Post irradiated	EWF annealing		300 deg C annealing
			5 Amp	80 A	
Saturation current	0.58 A	0.56 A	0.59 A	0.6 A	0.55 A
Maximum transconductance	0.277 S	0.268 S	0.292 S	0.286 S	
Leakage Current	4.42×10^{-10}	1.64×10^{-7}	3.96×10^{-7}	3.46×10^{-7}	6.06×10^{-7}
Threshold voltage	−2.75 V	−2.715 V	−2.73 V	−2.74 V	
Average FWHM (E_2 peak)	3.13	3.27	2.87		2.91

Currently, very little is known about the applicability of the EWF-based anneal on electronic devices. Therefore, future studies need to be dedicated to understanding the defect-electron interaction in electronics by performing parametric analysis of the EWF and device-specific parameters and also on devices subject to different types of radiation damage. In particular, it will be interesting to see if

displacement damage of the type produced by protons can also be mitigated by EWF annealing.

Acknowledgments

This work was funded by the Defense Threat Reduction Agency (DTRA) as part of the Interaction of Ionizing Radiation with Matter University Research Alliance (IIRM-URA) under contract number HDTRA1–20–2–0002. The content of the information does not necessarily reflect the position or the policy of the federal government, and no official endorsement should be inferred. AH also acknowledges support from the US National Science Foundation (ECCS # 2015795). The work at UF was also supported by NSF DMR 1856662 (James Edgar).

ORCID

Aman Haque https://orcid.org/0000-0001-6535-5484
Stephen Pearton https://orcid.org/0000-0001-6498-1256

References

1. M. Meneghini et al., *J. Appl. Phys.*, **130**, 181101 (2021).
2. J. He, W.-C. Cheng, Q. Wang, K. Cheng, H. Yu, and Y. Chai, *Adv. Electron. Mater.*, **7**, 2001045 (2021).
3. O. Ambacher, J. Smart, J. Shealy, N. Weimann, K. Chu, M. Murphy, W. Schaff, L. Eastman, R. Dimitrov, and L. Wittmer, *J. Appl. Phys.*, **85**, 3222 (1999).
4. A. Ionascut-Nedelcescu, C. Carlone, A. Houdayer, H. Von Bardeleben, J.-L. Cantin, and S. Raymond, *IEEE Trans. Nucl. Sci.*, **49**, 2733 (2002).
5. S. Liu, J. Zhang, S. Zhao, L. Shu, X. Song, C. Wang, T. Li, Z. Liu, and Y. Hao, *Appl. Phys. Lett.*, **120**, 202102 (2022).
6. S. Pearton, A. Aitkaliyeva, M. Xian, F. Ren, A. Khachatrian, A. Ildefonso, Z. Islam, M. A. J. Rasel, A. Haque, and A. Polyakov, *ECS J. Solid State Sci. Technol.*, **10**, 055008 (2021).
7. S. Vitusevich, N. Klein, A. Belyaev, S. Danylyuk, M. Petrychuk, R. Konakova, A. Kurakin, A. Rengevich, A. Y. Avksentyev, and B. Danilchenko, *physica status solidi (a)*, **195**, 101 (2003).
8. Z. Islam, A. L. Paoletta, A. M. Monterrosa, J. D. Schuler, T. J. Rupert, K. Hattar, N. Glavin, and A. Haque, *Microelectron. Reliab.*, **102**, 113493 (2019).
9. X. Hu, A. P. Karmarkar, B. Jun, D. M. Fleetwood, R. D. Schrimpf, R. D. Geil, R. A. Weller, B. D. White, M. Bataiev, and L. J. Brillson, *IEEE Trans. Nucl. Sci.*, **50**, 1791 (2003).
10. D. M. Fleetwood, E. X. Zhang, R. D. Schrimpf, and S. T. Pantelides, *IEEE Trans. Nucl. Sci.*, **69(5)**1105 (2022).
11. A. Yadav, E. Flitsiyan, L. Chernyak, Y.-H. Hwang, Y.-L. Hsieh, L. Lei, F. Ren, S. J. Pearton, and I. Lubomirsky, *Radiat. Eff. Defects Solids*, **170**, 377 (2015).
12. S. Cai, Y. Tang, R. Li, Y. Wei, L. Wong, Y. Chen, K. Wang, M. Chen, R. Schrimpf, and J. Keay, *IEEE Trans. Electron Devices*, **47**, 304 (2000).
13. A. Y. Polyakov, S. Pearton, P. Frenzer, F. Ren, L. Liu, and J. Kim, *J. Mater. Chem. C*, **1**, 877 (2013).
14. A. Yadav, C. Schwarz, M. Shatkhin, L. Wang, E. Flitsiyan, L. Chernyak, L. Liu, Y. Hwang, F. Ren, and S. J. Pearton, *ECS Trans.*, **61**, 171 (2014).
15. N. Shmidt, D. Davydov, V. Emtsev, I. Krestnikov, A. Lebedev, W. Lundin, D. Poloskin, A. Sakharov, A. Usikov, and A. Osinsky, *physica status solidi (b)*, **216**, 533 (1999).
16. B.-J. Kim, S. Ahn, F. Ren, S. J. Pearton, G. Yang, and J. Kim, *Journal of Vacuum Science & Technology B, Nanotechnology and Microelectronics: Materials, Processing, Measurement, and Phenomena*, **34**, 041231 (2016).
17. V. Emtsev, V. Y. Davydov, V. Kozlovskii, V. Lundin, D. Poloskin, A. Smirnov, N. Shmidt, A. Usikov, J. Aderhold, and H. Klausing, *Semicond. Sci. Technol.*, **15**, 73 (2000).
18. L. Polenta, Z. Fang, and D. C. Look, *Appl. Phys. Lett.*, **76**, 2086 (2000).
19. S. Jha, E. V. Jelenković, M. Pejović, G. Ristić, M. Pejović, K. Tong, C. Surya, I. Bello, and W. Zhang, *Microelectron. Eng.*, **86**, 37 (2009).
20. N. Miura, T. Nanjo, M. Suita, T. Oishi, Y. Abe, T. Ozeki, H. Ishikawa, T. Egawa, and T. Jimbo, *Solid-State Electronics*, **48**, 689 (2004).
21. G. Greco, F. Iucolano, S. Di Franco, C. Bongiorno, A. Patti, and F. Roccaforte, *IEEE Trans. Electron Devices*, **63**, 2735 (2016).
22. P. S. Ho and T. Kwok, *Rep. Prog. Phys.*, **52**, 301 (1989).
23. J. R. Black, *IEEE Trans. Electron Devices*, **16**, 338 (1969).
24. Z. Islam, A. Kozhakhmetov, J. Robinson, and A. Haque, *J. Electron. Mater.*, **49**, 3770 (2020).
25. G. Nelson and D. Reilly, *Passive Nondestructive Analysis of Nuclear Materials*, **2**, 27 (1991).
26. J. Kim, F. Ren, G. Chung, M. MacMillan, A. Baca, R. Briggs, D. Schoenfeld, and S. Pearton, *Appl. Phys. Lett.*, **84**, 371 (2004).
27. Y.-H. Hwang, Y.-L. Hsieh, L. Lei, S. Li, F. Ren, S. J. Pearton, A. Yadav, C. Schwarz, M. Shatkhin, and L. Wang, *Journal of Vacuum Science & Technology B, Nanotechnology and Microelectronics: Materials, Processing, Measurement, and Phenomena*, **32**, 031203 (2014).
28. J. Yang, G. J. Koller, C. Fares, F. Ren, S. Pearton, J. Bae, J. Kim, and D. J. Smith, *ECS J. Solid State Sci. Technol.*, **8**, Q3041 (2019).
29. J. H. Cahn, *J. Appl. Phys.*, **30**, 1310 (1959).
30. M. P. Khanal, B. Ozden, K. Kim, S. Uprety, V. Mirkhani, K. Yapabandara, A. C. Ahyi, and M. Park, *Journal of Vacuum Science & Technology B, Nanotechnology and Microelectronics: Materials, Processing, Measurement, and Phenomena*, **35**, 03D107 (2017).
31. C. Li and S. Subramanian, *IEEE Trans. Nucl. Sci.*, **50**, 1998 (2003).
32. S. Alshaikh, M. Carolan, M. Petasecca, M. Lerch, P. Metcalfe, and A. Rosenfeld, *Australas. Phys. Eng. Sci. Med.*, **37**, 311 (2014).
33. V. Danchenko, U. D. Desai, and S. S. Brashears, *J. Appl. Phys.*, **39**, 2417 (1968).
34. G. S. Ristić, *J. Phys. D: Appl. Phys.*, **42**, 135101 (2009).
35. C.-H. Chen, R. Sadler, D. Wang, D. Hou, Y. Yang, W. Yau, W. Sutton, J. Shim, S. Wang, and A. Duong, *Solid-State Electronics*, **126**, 115 (2016).
36. R. Vetury, N. Q. Zhang, S. Keller, and U. K. Mishra, *IEEE Trans. Electron Devices*, **48**, 560 (2001).
37. Z. Lin, H. Kim, J. Lee, and W. Lu, *Appl. Phys. Lett.*, **84**, 1585 (2004).
38. R. P. Khade, S. Sarkar, A. DasGupta, and N. DasGupta, *J. Appl. Phys.*, **130**, 205707 (2021).
39. Z. Kourdi, B. Bouazza, A. Guen-Bouazza, and M. Khaouani, *Microelectron. Eng.*, **142**, 52 (2015).
40. L. Lv, X. Ma, J. Zhang, Z. Bi, L. Liu, H. Shan, and Y. Hao, *IEEE Trans. Nucl. Sci.*, **62**, 300 (2015).
41. Y. Zeng, J. Ning, J. Zhang, Y. Jia, C. Yan, B. Wang, and D. Wang, *Applied Sciences*, **10(24)**, 8814 (2020).
42. S. Choi, E. Heller, D. Dorsey, R. Vetury, and S. Graham, *J. Appl. Phys.*, **113**, 093510 (2013).
43. S. Kushvaha, M. S. Kumar, K. Maurya, M. Dalai, and N. D. Sharma, *AIP Adv.*, **3**, 092109 (2013).